Scientific Research Publishing

Open Journal of Medicinal Chemistry, 2023, 13, 15-34
https://www.scirp.org/journal/ojmc
ISSN Online: 2164-313X
ISSN Print: 2164-3121

Synthesis, SAR, and in Silico ADME Screening Studies of Some 9-Amino-3-Phenylacridone Derivatives as Topoisomerase II Inhibitors

Abiodun S. Oyedele[1], Toluwase H. Fatoki[1,2], Esha Dalvie[3], Neil Osheroff[3,4,5], Cosmas O. Okoro[1*]

[1]Department of Chemistry, Tennessee State University, Nashville, Tennessee, USA
[2]Applied Bioinformatics Laboratory, Department of Biochemistry, Federal University Oye-Ekiti, Oye-Ekiti, Nigeria
[3]Departments of Biochemistry, Vanderbilt University School of Medicine, Nashville, Tennessee, USA
[4]Medicine (Hematology/Oncology), Vanderbilt University School of Medicine, Nashville, Tennessee, USA
[5]Vanderbilt Institute of Chemical Biology, Vanderbilt University School of Medicine, Nashville, Tennessee, USA

Email: *cokoro@tnstate.edu

How to cite this paper: Oyedele, A.S., Fatoki, T.H., Dalvie, E., Osheroff, N. and Okoro, C.O. (2023) Synthesis, SAR, and in Silico ADME Screening Studies of Some 9-Amino-3-Phenylacridone Derivatives as Topoisomerase II Inhibitors. *Open Journal of Medicinal Chemistry*, **13**, 15-34.
https://doi.org/10.4236/ojmc.2023.132002

Received: May 30, 2023
Accepted: June 27, 2023
Published: June 30, 2023

Abstract

Cancer is a leading cause of death globally, claiming about 9.6 million lives and approximately 420 million new cases of cancer will be diagnosed in the world by the year 2025. The aim of this study was to synthesize and computationally evaluate pharmacological potential of some derivatives of 9-amino-3-phenylacridone, as topoisomerase II (Topo II) inhibitors. In this study, 10 derivatives of 3-phenyl-9-aminoacridone were chemically synthesized and characterized, and the potential pharmacological indications of these compounds were computationally predicted by methods such as ADMET prediction, molecular target prediction and molecular docking. The results showed that two derivatives (58e and 58j) were non-permeant of blood-brain barrier, and this property was found similar to that of amsacrine and etoposide. The results of molecular docking of the ten derivatives of 3-phenyl-9-aminoacridone that were synthesized in this work showed that the synthetic compounds (58a-j) and the standard drugs have overall best binding affinities for human acetylcholine esterase than butyrylcholinesterase, and overall best binding affinities for human topo IIα than human topo IIβ. Overall, the results of this study suggest that the synthetic compounds 58a, 58c, 58f, 58g, and 58i could probably inhibit topo IIα by catalytic inhibition as seen with amsacrine, but only 58b and 58e possessed DNA non-intercalation properties as seen with etoposide, serving as topo II poison. In conclusion, this study showed that 3-phenyl-9-aminoacridone derivatives are potential inhibitor of topo IIα/β both by catalytic inhibition and poison as non-intercalator of DNA.

Keywords

Cancers, 9-Aminoacridone, Anticancer, Topoisomerase II, Pharmacokinetics, Molecular Docking, Etoposide

1. Introduction

Cancer is a disorder that results from genetic or epigenetic alterations in the somatic cells and has abnormal cell growth which may be spread to other body parts. They form a subset of neoplasm. The unregulated growth of cells in a group is called neoplasm or tumor and they form a lump or mass and may be distributed diffusely [1] [2]. Cancer is a leading cause of death globally (about 9.6 million deaths) and approximately 15 million new cancer cases will be diagnosed as the world population reached 7.5 billion by 2020 [3], and about 420 million new cases of cancer by 2025 [2]. Cancer cells utilize multiple strategies such as high glycolytic flux, redox signalling and modulation of autophagy to avoid cell death and overcome nutritional deficiency [4].

Topoisomerase (Topo) is an established target for anticancer drugs and is known to be responsible for regulating the topological constraints in DNA. Topo II inhibitors are classically divided into catalytic inhibitors and Topo II poisons, according to their mechanism of action. According to Okoro and Fatoki [5], topo II catalytic inhibitors destroy cancer cells through the inhibitions of Topo II enzymatic activities, thus preventing the formation of topo II-DNA complex without increasing DNA cleavage, via the mechanisms of action that include interfering with DNA binding, inhibiting cleavage of the DNA molecule, ATP hydrolysis, and binding to the ATP binding site, whereas Topo II poisons destroy cancer cells by increasing the amount of covalent Topo II-DNA complexes and preventing the religation of the cleaved DNA strands, thus forming unwanted double strand breaks that are toxic to the cells, and, subsequently, leading to apoptosis.

Most of the first-line agents for treating cancer are Topo II poisons, such as etoposide (non-intercalator), doxorubicin, and m-amsacrine (intercalator), but due to side effects, such as risk of cardiotoxicity and secondary malignancies, that are often encountered during the use of DNA poisonous drugs, research is now shifting towards the discovery of Topo II catalytic inhibitors, which have good pharmacokinetics profiles [5].

In silico approaches that involve virtual high-throughput screening (VHTS), three-dimensional quantitative structure activity and relationship (3D-QSAR), molecular docking, and ADME/Tox prediction have been applied to study potential inhibitors of Topo IIα [6] [7]. The present study builds on the previous report from our lab on some acridone derivatives [8]. The aim of this study was to synthesize and computationally evaluate pharmacological potential of some derivatives of 9-amino-3-phenylacridone, as topoisomerase II inhibitors.

2. Materials and Methods

2.1. Organic Synthesis

General procedure for the synthesis 9-aminoacridone derivatives containing 3-Phenyl group synthesis (58a-58j)

STEP I: 5-substituted-1,3-cyclohexanedione (1.5 mmol) and 2-amino-4,5-substituted-benzonitrile (1.5 mmol) were suspended in a diluted aqueous solution of hydrochloric acid (60 mmol, 50 - 60 ml) at 80˚C - 90˚C. At the end of the reaction (progress monitored by TLC), the reaction mixture was cooled, filtered, and washed thoroughly with water.

STEP II: To a round-bottomed flask containing 10 ml of tetrahydrofuran (THF), cuprous chloride (0.0165 g, 0.167 mmol) and potassium carbonate (0.046 g, 0.333 mmol), 5-substituted enaminone (1 mmol) wad added and the reaction mixture was refluxed for the indicated time (~6 h) (monitored by TLC). The hot mixture was filtered into hexane, wherein precipitate separated and filtered off to get moderate to good yield acridone derivatives with 3-phenyl and 9-amino groups (Figure 1).

9-amino-7-chloro-3-phenyl-3,4-dihydroacridin-1(2H)-one (58a) Light Yellow solid, mp = 250˚C - 252˚C. IR (neat) 3311, 3169, 2959, 1609, 828 cm^{-1}; ^{1}H NMR (DMSO) δ 2.0 - 2.2 (m, 2H), 2.4 - 2.8 (m, 2H), 3.0 - 3.5 (m, 2H), 7.0 - 7.5 (d, 5H), 7.5 - 8.0 (d, 2H), 8.5 - 8.7 (d, 2H), 10 (br, s, 1H). ^{13}C (400 MHz, DMSO) δ 200.43, 163.60, 154.29, 144.09, 132.66, 130.97, 129.37, 129.01, 127.32, 123.21, 119.9, 105.72, 46.54, 41.66, 40.62, 40.20, 39.78, 38.58.

9-amino-7-bromo-3-phenyl-3,4-dihydroacridin-1(2H)-one (58b) Light Yellow solid, mp = 257˚C - 259˚C. IR (neat) 3334, 3175, 2950, 1640, 829 cm^{-1}; ^{1}H NMR (DMSO) δ 2.0 - 2.2 (m, 2H), 2.4 - 2.8 (m, 2H), 3.0 - 3.5 (m, 2H), 7.0 - 7.5 (d, 5H), 7.5 - 8.0 (d, 2H), 8.5 - 8.7 (d, 2H) 10 (br, s, 1H). ^{13}C (400 MHz, DMSO) δ 200.54, 163.81, 154.23, 146.96, 143.87, 135.46, 130.79, 129.06, 127.31, 127.13,

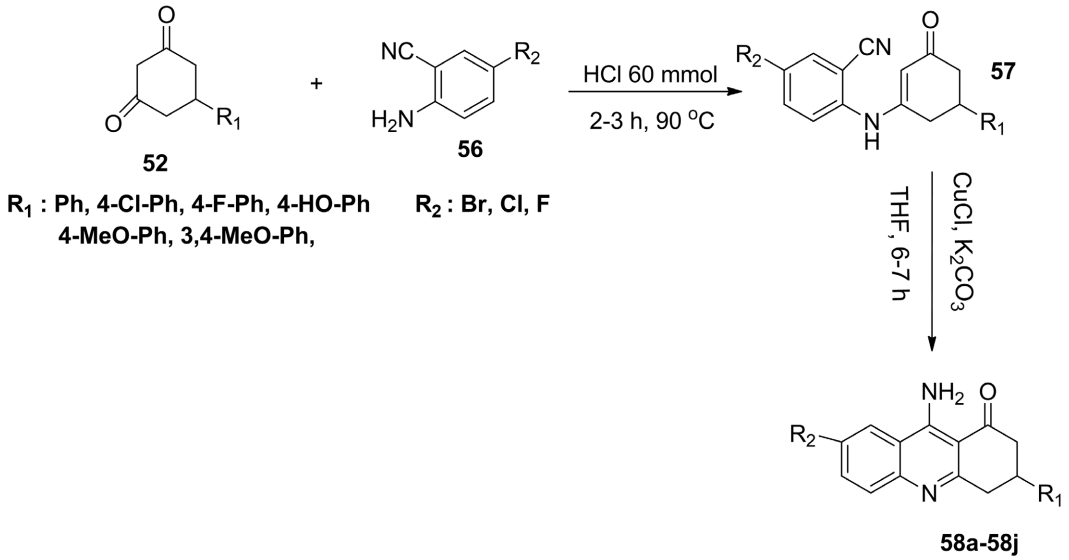

Figure 1. Synthesis of 3-phenyl-9-aminoacridone derivatives.

126.20, 119.93, 117.79, 105. 71, 36.41, 41.38, 40.24, 39.82, 39.20, 38.50.

9-amino-7-fluoro-3-phenyl-3,4-dihydroacridin-1(2H)-one (58c) Light Yellow solid, mp = 280˚C - 281˚C. IR (neat) 3318, 3162, 2953, 1619, 841 cm-1; ^{1}H NMR (DMSO) δ 2.0 - 2.2 (m, 1H), 2.4 - 2.8 (m, 2H), 3.0 - 3.3 (m, 3H), 7.0 - 7.5 (d, 6H), 7.5 - 8.0 (d, 2H), 8.0 - 8.5 (d, 2H), 10 (br, s, 1H). ^{13}C (400 MHz, DMSO) δ 200.51, 162.50, 145.47, 144.08, 131.39, 129.02, 127.32, 127.06, 121.56, 108.31, 108.08, 105.35, 46.55, 41.50, 40.51, 40.30, 39.67, 39.46, 38.63.

9-amino-7-chloro-3-(4-methoxyphenyl)-3,4-dihydroacridin-1(2H)-one (58d) Light Yellow solid, mp = 259˚C - 260˚C. IR (neat) 3306, 3168, 2996, 1609, 830 cm^{-1}; ^{1}H NMR (DMSO) δ 2.0 - 2.2 (m, 1H), 2.5 - 3.0 (m, 1H), 3.0 - 3.5 (m, 5H), 3.6 - 3.8 (4H), 6.8 - 7.5 (d, 4H), 7.5 - 8.0 (d, 2H), 8.3 - 8.6 (d, 2H), 10 (br, s, 1H). ^{13}C (400 MHz, DMSO) δ 200, 163.68, 158.39, 154.26, 136.05, 132.62, 130.96, 129.34, 128.28, 123.19, 119.48, 114.38, 105.74, 55.50, 46.83, 41.93, 40.43, 39.59, 37.78.

9-amino-7-chloro-3-(3,4-dimethoxyphenyl)-3,4-dihydroacridin-1(2H)-one (58e) Light Yellow solid, mp = 255˚C - 257˚C. IR (neat) 3324, 3171, 2943, 1608, 831 cm^{-1}; ^{1}H NMR (DMSO) δ 2.0 - 2.2 (1H), 2.5 - 2.8 (m, 1H), 2.8 - 3.3 (m, 3H), 3.3 - 3.6 (m, 1H), 3.6- 3.8 (7H), 6.7 - 7.3 (d, 2H), 7.5 - 7.8 (d, 2H), 8.3 - 8.7 (d, 2H), 10 (br, s, 1H). ^{13}C (400 MHz, DMSO) δ 163.73, 111.55, 56.01, 40.64, 40.43, 40.02, 39.81, 39.60, 39.39.

9-amino-7-chloro-3-(4-chlorophenyl)-3,4-dihydroacridin-1(2H)-one (58f) Light Yellow solid, mp = 284˚C - 285˚C. IR (neat) 3312, 3168, 2875, 1609, 828 cm^{-1}; ^{1}H NMR (DMSO) δ 2.0 - 2.2 (m, 2H), 2.4 - 2.8 (m, 2H), 3.0 - 3.4 (m, 1H), 7.6 - 7.8 (d, 6H), 8.5 - 8.6 (d, 2H), 10 (br, s, 1H). ^{13}C (400 MHz, DMSO) δ 200.17, 163.40, 154.31, 147.00, 143.05, 132.72, 131.62, 130.92, 129.45, 129.30, 128.98, 123.18, 105.68, 46.28, 41.36, 40.35, 40.14, 39.93, 39.51, 39.30, 37.97.

9-amino-7-chloro-3-(4-fluorophenyl)-3,4-dihydroacridin-1(2H)-one (58g) Light Yellow solid, mp = 300˚C - 301˚C. IR (neat) 3311, 3168, 2960, 1608, 828 cm^{-1}; ^{1}H NMR (DMSO) δ 2.0 - 2.2 (m, 1H), 2.6 - 3.0 (m, 1H), 3.0 - 3.3 (m, 5), 7.0 - 7.3 (d, 4H), 7.5 - 7.8 (d, 4H), 8.5 - 8.7 (d, 4H), 10 (br, s, 1H). ^{13}C (400 MHz, DMSO) δ 200.30, 163.50, 154.31, 147.01, 140.25, 132.70,130.92, 129.43, 129.43, 129.24, 129.17, 123.18, 119.47, 115.78, 115.57, 105.68, 46.57, 41.65, 40.56, 40.14, 39.51, 37.86.

9-amino-7-bromo-3-(4-chlorophenyl)-3,4-dihydroacridin-1(2H)-one (58h) Yellow solid, mp = 281˚C - 282˚C. IR (neat) 3350, 3176, 2952, 1603, 828 cm^{-1}; ^{1}H NMR (DMSO) δ 2.0 - 2.5 (m, 7H), 2.5 - 3.4 (m, 4H), 6.8 - 7.8 (d, 4H), 7.5 - 8.0 (8H), 8.4 - 8.7 (d, 2H), 10 (br, s, 1H). ^{13}C (400 MHz, DMSO) δ 200.15, 163.50, 154.22, 147.21, 143.04, 135.3, 131.62, 131.05, 129.30, 129.20, 128.58, 126.33, 120.02, 117.69, 46.27, 41.39, 40.55, 40.13, 39.92, 39.51, 39.30, 37.95.

9-amino-3-(4-chlorophenyl)-7-fluoro-3,4-dihydroacridin-1(2H)-one (58i) Yellow solid, mp = 298˚C - 299˚C. IR (neat) 3294, 3152, 2953, 1620, 829 cm^{-1}; ^{1}H NMR (DMSO) δ 2.0 - 2.3 (1H), 2.6 - 3.3 (m, 4H), 7.2 - 7.8 (7H), 8.0 - 8.6 (d, 2H), 10 (br, s, 1H). ^{13}C (400 MHz, DMSO) δ 200.20, 162.26, 160.49, 154.59, 145.50, 143.10, 131.61, 131.43, 129.30, 128.93, 121.81, 121.56, 119.02, 108.35, 108.12,

105.31, 46.33, 41.31, 40.15, 39.94, 39.52, 38.04.

9-amino-7-chloro-3-(4-hydroxyphenyl)-3,4-dihydroacridin-1(2H)-one (58j) Light Yellow solid, mp = 299˚C - 300˚C. IR (neat) 3201, 1613, 827 cm^{-1}; ^{1}H NMR (DMSO) δ 2.0 - 2.3 (1H), 2.3 - 2.7 (m, 1H), 6.3 - 6.8 (d, 2H), 7.0 - 7.3 (d, 2H), 7.5 - 7.8 (2H), 8.3 - 8.6 (d, 2H), 10 (br, s, 1H). ^{13}C (400 MHz, DMSO) δ 195.66, 162.65, 162.08, 160.24, 140.97, 140.20, 135.01, 133.78, 130.73, 129.38, 129.30, 129.04, 115.92, 115.76, 115.55, 110.61, 100.05, 44.41, 40.56, 40.35, 39.93, 39.72, 38.92, 35.68.

5.9 Procedure for dealkylation of 5-(4-methoxyphenyl)cyclohexane-1,3-dione (X) by BBr3 for the synthesis of 9-amino-7-chloro-3-(4-hydroxyphenyl)-3,4-dihydroacridin-1(2H)-one 58j

The treatment of **X** with BBr_3 for 4 h at r.t. in 0.4 M dry methylenechloride under the condition of **X**: BBr3 = 1:0.7 mol/mol gave the optimal yield of 5-(4-hydroxyphenyl)cyclohexane-1,3-dione **Y.**[153] **Y** became a lead compound for the synthesis of **58j** following Shutskee's method.

IR (neat) 3201, 1613, 1498, 827 cm^{-1}; ^{1}H NMR (DMSO) δ 2.2 - 2.6 (d, 3H), 2.6 - 2.8 (d, 1H), 3.0 - 3.5 (d, 1H), 5.2 - 5.4 (br, s, 1H), 6.5 - 6.9 (dd, 1H), 7.0 - 7.3 (dd, 1H). ^{13}C (400 MHz, DMSO) δ 156.37, 134.25, 128.23, 115.60, 103.96, 40.54, 40.33, 40.13, 39.71, 39.50, 39.29, 38.46.

2.2. Computational Studies

2.2.1. Ligand Preparation

The structures of 10 synthetic compounds (ligands) were designed using ACD-Labs/ChemSketch software, and saved as SMILES formats. Also, 2 standard compounds (etoposide and amsacrine) were included in this study.

2.2.2. *In Silico* Pharmacokinetics

The SMILES of each of the ligands were used for *in silico* ADME (absorption, distribution, metabolism, and excretion) screening on SwissADME server [9], which was performed at default parameters. Also, the ADMET (Absorption, Distribution, Metabolism, Excretion, and Toxicity) studies were calculated using the pkCSM server (http://biosig.unimelb.edu.au/pkcsm/, [10]).

2.2.3. *In-Silico* Target Prediction

Ligands SMILES were used for target prediction on STITCH webserver v5.0 (http://www.stitch.embl.de/) [11], where *Homo sapiens* was designated as target organism.

2.2.4. Molecular Docking Studies

The molecular docking studies were carried out according to the method of Fatoki *et al.* [12]. Briefly, human topoisomerases II (Topo IIα and Topo IIβ), human acetylcholinesterase and human butyrylcholinesterase were obtained from the http://www.rcsb.org/pdb with PDB ID: 1zxm and 3qx3, as well as human acetylcholinesterase and butyrylcholinesterase with PDB ID: 1b41 and 6qac respectively. The ligand structures were subjected to 3D structure optimization

using ACDLab/Chemsketch software, and were saved in.mol format. PyMol software was used for ligand file conversion from.mol to.pdb and for the preparation of protein chain A with removal of water and existing ligands. Both ligand and protein were prepared for docking using AutoDock Tools (ADT) v1.5.6 [13] at default settings, and the output file was saved in pdbqt format. Docking parameters used were: center grid box (39.930 × 2.419 × 25.562 points), size (110 × 114 × 126 points), and spacing (0.575 Å) for human Topo IIα (PDB ID: 1ZXM); center grid box (27.870 × 114.839 × 68.155 points), size (116 × 126 × 90 points), and spacing (0.775 Å) for human Topo IIβ (PDB ID: 3QX3); center grid box (16.751 × 31.857 × 38.786 points), size (126 × 126 × 126 points) and spacing (0.514 Å) for human butyrylcholinesterase (PDB ID: 6QAC); and center (116.412 × 104.282 × -142.677 points); size (126 × 126 × 126 points) and spacing (0.514 Å) for human acetylcholinesterase (PDB ID: 1B41). Molecular docking program AutoDock Vina v1.2.3 [14] [15] was employed for the docking experiment. After docking, close interactions of binding of the target with the ligands were analyzed and visualized on ezLigPlot available in ezCADD server [16].

3. Results

The molecular weight of the ten derivatives of 3-phenyl-9-aminoacridone that were synthesized in this work have molecular weights ranging from 306.33 g/mol (58c) to 382.84 g/mol (58e); with melting points ranging between 250 C (58a) to 301 (58g), as shown in **Table 1**. The structure of the ten derivatives of 3-phenyl-9-aminoacridone together with standard drugs, amsacrine and etoposide, are shown in **Figure 2**.

All the 10 derived compounds have moderate solubility, high gastrointestinal absorption and inhibitory effect on cytochromes which are similar to that of amsacrine. Two derivatives (58e and 58j) were predicted to be non-permeant of

Table 1. Physical and Chemical Properties of 58a-58j.

Entry	Compounds	R_1	R_2	Time (h)	Molecular Weight	Melting point (˚C)
1	58a	Ph	Cl	6	322.79	250 - 252
2	58b	Ph	Br	6	367.24	257 - 259
3	58c	Ph	F	6	306.33	280 - 281
4	58d	4-MeO-Ph	Cl	6	352.81	259 - 260
5	58e	3,4-MeO-Ph	Cl	6	382.84	255 - 257
6	58f	4-Cl-Ph	Cl	6	357.23	284 - 285
7	58g	4-F-Ph	Cl	6	340.78	300 - 301
8	58h	4-Cl-Ph	Br	6	401.68	281 - 282
9	58i	4-Cl-Ph	F	6	340.78	298 - 299
10	58j	4-OH-Ph	Cl	6	338.79	299 - 300

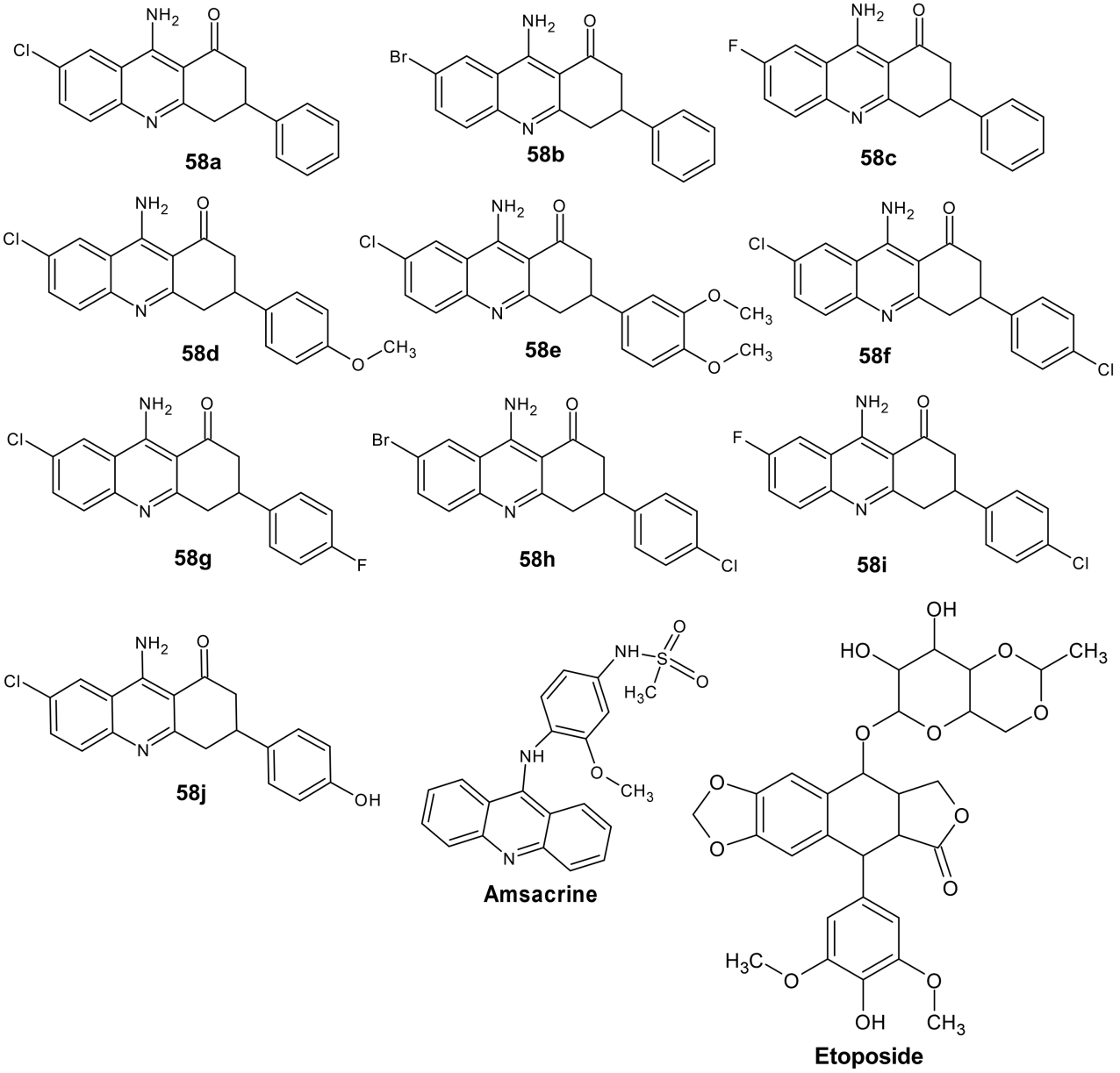

Figure 2. Structure of the synthetic compounds 58a-58j and standard drugs (amsacrine and etoposide).

blood-brain barrier, and this property was found similar to that of amsacrine and etoposide, as indicated in Table 2. Furthermore, ADMET results in Table 3 indicate that the intestinal absorption of compounds 58e was predicted to be slightly higher than that of amsacrine and etoposide, and that all the synthetic compounds have intestinal absorption that are much higher than that of etoposide. Also, all the synthetic compounds as well as amsacrine and etoposide were predicted to be inhibitors of p-glycoprotein I and II. The results indicate that compounds 58d-i have cytochrome P450 inhibitory profiles that are similar to that of amsacrine. The toxicity results showed that only compound 58e has no AMES toxicity potential, which is similar to that of etoposide, and that only etoposide was not a potential inhibitor of hERG II with no potential hepatotoxicity.

Table 2. Predicted pharmacokinetics properties of selected ligands.

SN	Ligands	Predicted ADME Parameter from SWISSADME												
		MW	MR	TPSA (Å²)	Log P	ESOL Log S	ESOL Class	GIA	BBB permeant	P-gp	CYPs Inhibitor	Log Kp (cm/s)	BS	SA
1	58a	322.79	93.5	55.98	3.81	−4.95	Moderately soluble	High	Yes	Yes	CYP1A2, CYP2C19, CYP2C9, CYP3A4	−5.27	0.55	3.07
2	58b	367.24	96.19	55.98	3.9	−5.26	Moderately soluble	High	Yes	Yes	CYP1A2, CYP2C19, CYP2C9, CYP3A4	−5.5	0.55	3.09
3	58c	306.33	88.45	55.98	3.58	−4.51	Moderately soluble	High	Yes	Yes	CYP1A2, CYP2C19, CYP3A4	−5.55	0.55	3.07
4	58d	352.81	99.99	65.21	3.80	−5.01	Moderately soluble	High	Yes	Yes	CYP1A2, CYP2C19, CYP2C9, CYP3A4	−5.48	0.55	3.14
5	58e	382.84	106.48	74.44	3.77	−5.07	Moderately soluble	High	No	Yes	CYP1A2, CYP2C19, CYP2C9, CYP3A4	−5.68	0.55	3.35
6	58f	357.23	98.51	55.98	4.33	−5.53	Moderately soluble	High	Yes	Yes	CYP1A2, CYP2C19, CYP2C9, CYP3A4	−5.04	0.55	3.09
7	58g	340.78	93.46	55.98	4.11	−5.1	Moderately soluble	High	Yes	Yes	CYP1A2, CYP2C19, CYP2C9, CYP3A4	−5.31	0.55	3.08
8	58h	401.68	101.2	55.98	4.41	−5.85	Moderately soluble	High	Yes	Yes	CYP1A2, CYP2C19, CYP2C9, CYP3A4	−5.26	0.55	3.09
9	58i	340.78	93.46	55.98	4.12	−5.1	Moderately soluble	High	Yes	Yes	CYP1A2, CYP2C19, CYP2C9, CYP3A4	−5.31	0.55	3.08
10	58j	338.79	95.52	76.21	3.37	−4.8	Moderately soluble	High	No	Yes	CYP1A2, CYP2C19, CYP2C9, CYP2D6, CYP3A4	−5.63	0.55	3.05
11	Amsacrine	393.46	113.55	88.7	3.47	−5	Moderately soluble	High	No	No	CYP1A2, CYP2C19, CYP2C9, CYP2D6, CYP3A4	−5.85	0.55	2.94
12	Etoposide	588.56	139.11	160.83	1.15	−3.75	Soluble	Low	No	Yes	CYP2D6	−9.46	0.17	6.27

Note: Physicochemical properties: Molecular weight (MW), Molar Refractivity (MR), Total polar surface area (TPSA). **Lipophilicity**: Consensus Log P. **Water Solubility:** ESOL Log S, ESOL Class. **Pharmacokinetics:** Gastrointestinal absorption (GIA), Blood-brain barrier (BBB), P-glycoprotein (P-gp) substrate, Inhibition of Cytochrome P450 (CYPs) type CYP1A2, CYP2C19, CYP2C9, CYP2D6, and CYP3A4, Skin permeation (Log Kp). **Druglikeness**: Bioavailability Score (BS), **Medicinal Chemistry:** Synthetic accessibility (SA).

Table 3. The ADMET profile of the selected lead compounds.

ADMET		COMPOUNDS											
Type	**Properties**	**58a**	**58b**	**58c**	**58d**	**58e**	**58f**	**58g**	**58h**	**58i**	**58j**	**Amsc**	**Etop**
Absorption	Water solubility (log mol/L)	−4.358	−4.426	−4.179	−4.754	−5.034	−5.125	−4.855	−5.203	−4.669	−4.392	−4.889	−3.487
	Caco-2 permeability (log Papp in 10 cm/s)	1.367	1.373	1.335	1.150	1.193	1.253	1.372	1.251	1.371	0.593	0.579	0.403
	Intestinal absorption (human) (% Absorbed)	94.024	93.957	94.926	92.892	95.07	91.044	91.946	90.977	92.036	89.82	94.938	75.614
	Skin Permeability (log Kp)	−2.787	−2.786	−2.79	−2.817	−2.832	−2.876	−2.883	−2.874	−2.807	−2.917	−2.734	−2.735
	P-glycoprotein substrate	No	No	No	No	No	Yes	Yes	Yes	Yes	Yes	Yes	Yes
	P-glycoprotein I inhibitor	Yes	Yes	Yes	Yes	Yes	Yes	Yes	Yes	Yes	Yes	Yes	Yes
	P-glycoprotein II inhibitor	Yes	Yes	Yes	Yes	Yes	Yes	Yes	Yes	Yes	Yes	Yes	Yes
Distribution	VDss (human) (log L/kg)	−0.007	0.012	−0.157	0.032	0.038	0.170	0.012	0.189	0.092	−0.028	−0.987	−0.218
	Fraction unbound (human)	0.028	0.025	0.042	0.052	0.061	0.046	0.066	0.043	0.079	0.078	0.120	0.038
	BBB permeability (log BB)	−0.006	−0.007	−0.013	−0.006	−0.423	0.122	0.115	0.120	0.154	−0.164	−0.096	−1.567
	CNS permeability (log PS)	−1.522	−1.499	−1.676	−1.664	−1.871	−1.365	−1.519	−1.343	−1.546	−1.670	−2.200	−4.115
Metabolism	CYP2D6 substrate	No	No	No	No	No	No	No	No	No	No	No	No
	CYP3A4 substrate	No	No	No	Yes	Yes	Yes	Yes	Yes	Yes	Yes	Yes	Yes
	CYP1A2 inhibitor	Yes	Yes	Yes	Yes	Yes	Yes	Yes	Yes	Yes	Yes	Yes	No
	CYP2C19 inhibitor	Yes	Yes	Yes	Yes	Yes	Yes	Yes	Yes	Yes	Yes	Yes	No
	CYP2C9 inhibitor	Yes	Yes	Yes	Yes	Yes	Yes	Yes	Yes	Yes	Yes	Yes	No
	CYP2D6 inhibitor	No	No	No	No	No	No	No	No	No	No	No	No
	CYP3A4 inhibitor	Yes	Yes	Yes	Yes	Yes	Yes	Yes	Yes	Yes	No	Yes	No
Excretion	Total Clearance (log ml/min/kg)	0.116	0.094	−0.042	0.141	0.276	−0.017	−0.035	−0.039	−0.028	−0.004	0.246	−0.068
	Renal OCT2 substrate	No	No	No	No	No	No	No	No	No	No	No	No
Toxicity	AMES toxicity	Yes	Yes	Yes	Yes	No	Yes	Yes	Yes	Yes	Yes	Yes	No
	Max. tolerated dose (human) (log mg/kg/day)	0.254	0.254	0.236	−0.008	0.063	−0.011	−0.039	−0.01	0.085	−0.093	0.266	0.171

Continued

hERG I inhibitor	No	No	No	No	No	No	No	No	No	No	No	No
hERG II inhibitor	Yes	Yes	Yes	Yes	Yes	Yes	Yes	Yes	Yes	Yes	Yes	No
Oral Rat Acute Toxicity (LD50) (mol/kg)	2.743	2.752	2.701	2.797	2.812	2.948	2.910	2.955	2.777	2.879	1.960	3.250
Oral Rat Chronic Toxicity (LOAEL) (log mg/kg_bw/day)	1.118	1.092	1.243	1.585	1.481	1.011	1.163	0.983	1.702	1.258	1.400	2.429
Hepatotoxicity	Yes	Yes	Yes	Yes	Yes	Yes	Yes	Yes	Yes	Yes	Yes	No
Skin Sensitisation	No	No	No	No	No	No	No	No	No	No	No	No
T. Pyriformis toxicity (log ug/L)	0.393	0.392	0.395	0.424	0.388	0.513	0.563	0.512	0.427	0.479	0.287	0.285
Minnow toxicity (log mM)	0.207	0.061	0.541	−0.236	−1.443	0.064	0.397	−0.082	0.555	0.722	−0.078	2.217

Also, compound 58f-h was predicted to have highest *T. Pyriformis* toxicity.

The protein targets of the ten derivatives of 3-phenyl-9-aminoacridone that were synthesized in this work includes acetylcholinesterase (ACHE), butyrylcholinesterase (BCHE), carboxylesterase 4A/5A/1 (CES4A/CES5A/CES1), carboxyl ester lipase (CEL), and neuroligin 1 (NLGN1). These targets did not match any of targets of amsacrine and etoposide (**Table 4**).

The results of molecular docking of the ten derivatives of 3-phenyl-9-aminoacridone that were synthesized in this work, showed that the synthetic compounds (58a-j) and the standard drugs have overall best binding affinities for human acetylcholine esterase than butyrylcholinesterase, and overall best binding affinities for human topo IIα than human topo IIβ as shown in **Table 5**. The docking pose of interaction of some of the compounds with the molecular targets are presented in **Figure 3** and **Figure 4**, which indicated the involvement of hydrogen bonding and pi-stacking in some of the ligand-protein complexes.

4. Discussion

Ten derivatives of 3-phenyl-9-aminoacridone were synthesized in this work. The results of the ADMET in this study indicate that compounds 58a-j have profiles that are nearly identical to that of amsacrine. The results of molecular target prediction pointed the compounds 58a-j towards acetylcholinesterase (AChE), butyrylcholinesterase, carboxyl ester lipase, and neuroligin 1 proteins.

Neuroligin 1 (NLGN1) encodes a trans-synaptic protein that acts as a postsynaptic adhesion molecule involved in the regulation of glutamatergic transmission. A study has shown that increased mRNA and protein levels of NLGN1 expression were associated with worse overall survival or recurrence-free survival in colorectal cancer patients [17]. Moreover, it was found that Neuroligin 1

Table 4. Predicted protein targets of the synthetic compounds and standard drugs.

SN	Ligands	% Probability of Predicted Targets														
		A	B	C	D	E	F	G	H	I	J	K	L	M	N	O
1	58a	86.9	79.3	56.1	56.1	56.1										
2	58b	67.1	48.2													
3	58c	82.5	65.9													
4	58d	86.9	79.3	56.1	56.1	56.1										
5	58e	86.9	79.3	56.1	56.1	56.1										
6	58f	90.6	79.3	56.1	56.1	56.1										
7	58g	86.9	79.3	56.1	56.1	56.1										
8	58h	90.6	69.8	51.7	51.7	51.7										
9	58i	90.6	69.8	51.7	51.7	51.7										
10	58j	86.9	79.3	56.1	56.1	56.1										
11	Amsacrine						99.4	99.2	93.8	88.1	80.0	73.9	70.0	70.0	70.0	
12	Etoposide															43.4

Note: A: Acetylcholinesterase (ACHE). **B**: Butyrylcholinesterase (BCHE). **C**: Carboxylesterase 4A/5A/1 (CES4A/CES5A/CES1). **D**: Carboxyl ester lipase (CEL) **E**: Neuroligin 1 (NLGN1) **F**: Topoisomerase (DNA) II beta (TOP2B). **G**: Topoisomerase (DNA) II alpha (TOP2A). **H**: Tumor protein p53 (TP53). **I**: Potassium voltage-gated channel, subfamily H (eag-related), member 2 (KCNH2). **J**: matrix metallopeptidase 2 (MMP2). **K**: Topoisomerase (DNA) I (TOP1). **L**: B-cell CLL/lymphoma 2 (BCL2). **M**: Caspase 2, apoptosis-related cysteine peptidase (CASP2). **N**: Werner syndrome, RecQ helicase-like (WRN). **O**: UDP-galactose-4-epimerase (GALE).

Table 5. Molecular docking parameters with binding free energy of the acridone compounds to topoisomerases.

SN	COMPOUND (LIGANDS)	Binding Affinity (kcal/mol)			
		Human topoisomerase IIα (PDB ID: 1ZXM)	Human topoisomerase IIβ (PDB ID: 3QX3)	Human acetylcholinesterase (PDB ID: 1B41)	Human butyrylcholinesterase (PDB ID: 6QAC)
1	58a	−7.772 H−Bond: Ser320 Interacting residues: Trp62, Tyr72, Arg241, Lys306, Gln310	−8.140 Interacting residues: Arg688, Arg692, Ser733, Phe1019	−7.115 Interacting residues: Ile471, Arg475, Tyr479, Asn490, Glu491, Ala497	−8.933 Interacting residues: Trp82, Gly116, Gly117, Thr120, Ser198, Asn289, His438, Gly439
2	58b	−7.380 Interacting residues: Pro111, Lys233, Val236, Leu257, Asn258, Asn260	−7.016 Interacting residues: Pro802, Ile803, Gly804, Val1194	−9.410 Interacting residues: Tyr124, Trp286, Phe295, Phe338, Tyr341	−8.681 Interacting residues: Gly116, Gly117, Thr120, Ser198, Asn289, His438, Gly439
3	58c	−7.160 Interacting residues: Trp62, Tyr72, Ile311, Ser312, Ser320	−8.432 Interacting residues: Arg688, Arg689, Arg743, Phe1019, Gly1023	−9.489 Interacting residues: Tyr124, Trp286, Phe295, Phe338, Tyr341	−7.530 Interacting residues: Asn228, Pro230, Val233, Pro303, Tyr396, Trp522

Continued

4	58d	−8.625 H−Bond: Tyr64 Interacting residues: Glu66, Asp232, Val236, Val240	−7.321 H−Bond: Gln995 Interacting residues: Leu969, Met959, Lys992, Lys1006	−8.423 Interacting residues: Tyr72, Tyr124, Trp286, Tyr337, Phe338, Tyr341	−8.744 H−Bond: Asn289 Interacting residues: Asp70, Trp82, Thr120, Asn289, Ala328, Trp430
5	58e	−8.211 H−Bond: Tyr64 Interacting residues: Glu66, Val236, Val240, Tyr244	−7.164 Interacting residues: Asn790, Pro802, Phe806, Val1194	−8.928 Interacting residues: Tyr124, Trp286, Phe295, Tyr337, Phe338, Tyr341	−7.973 Interacting residues: Glu238, Asn241, Arg242, Tyr282, Thr284, Leu286, Pro359, Asn397
6	58f	−7.871 Interacting residues: Trp62, Tyr72, Lys306, Gln310, Arg241	−7.105 Interacting residues: Ser725, Glu728, Arg729, Pro740, His774, His775	−8.052 Interacting residues: Tyr72, Trp286, Phe338, Tyr341	−8.731 Interacting residues: Asn228, Asp304, Glu308, Pro401, Glu404, Lys408, Trp522, Thr523
7	58g	−8.843 H−Bond: Tyr64 Interacting residues: Asp65, Glu66, Lys233, Val236, Val240, Leu257	−7.488 Interacting residues: Glu728, Pro740, Leu845, Glu855, Trp856, Phe1019	−9.498 Interacting residues: Tyr124, Trp286, Tyr337, Phe338, Tyr341	−7.908 Interacting residues: Arg242, Tyr282, Thr284, Leu286, Tyr396
8	58h	−8.482 Interacting residues: Tyr64, Glu66, Val236, Tyr244, Leu257, Asn260,	−7.239 Interacting residues: Ala663, Leu667, Asp676, Trp680, Asn683	−9.128 Interacting residues: Tyr124, Trp286, Leu289, Phe397, Phe338, Tyr341	−8.726 Interacting residues: Asn68, Trp82, Thr120, Asn289, Trp430, Tyr440, Met437
9	58i	−7.431 Interacting residues: Gln59, Met61, Tyr72, Tyr82, Ser320	−7.237 Interacting residues: Pro958, Thr966, Leu969, Gln995, Ala999, Val1004	−9.358 Interacting residues: Tyr124, Trp286, Leu289, Tyr337, Phe338, Tyr341	−7.071 Interacting residues: Tyr396, Trp522, Phe526
10	58j	−8.622 H−Bond: Tyr64 Interacting residues: Asp65, Glu66, Val236, Val240, Tyr244	−7.148 Interacting residues: Ala663, Leu667, Trp680, Asn683	−9.126 Interacting residues: Tyr124, Trp286, Gln291, Glu292, Phe338, Tyr341	−9.147 Interacting residues: Trp82, Thr120, Pro285, Asn289, Ala328, His438
11	Amsacrine	−8.663 Interacting residues: Met61, Trp62, Tyr72, Tyr82, Arg241, Asp245, Tyr274, Lys306, Gln310, Ile311, Ser320	−7.546 Interacting residues: Ser733, Pro740, Arg743, Phe1019	−9.436 Interacting residues: Tyr72, Tyr124, Trp286, Leu289, Glu292, Val294, Phe295, Arg296, Phe338, Tyr341	−9.936 Interacting residues: Trp82, Thr120, Ala328,
12	Etoposide	−8.342 H−Bond: Gln310 Interacting residues: Met61, Trp62, Phe308, Gln310, Ser320, Lys321, Gly322, Gly323, Val326	−9.067 H−Bond: Asp1201 Interacting residues: Asn790, Gln801, Pro802, Ile803, Gly804, Gln805, Phe806, Thr808, Ser827, Val1194, Gln1197	−9.571 H−Bond: Arg247 Interacting residues: Pro235, Thr238, Val239, Arg247, Leu289, Pro290, Arg296, Gln369, His405, Trp532, Pro537	−9.277 H−Bond: Tyr396 Interacting residues: Pro230, Val233, Glu238, Tyr396, Pro527

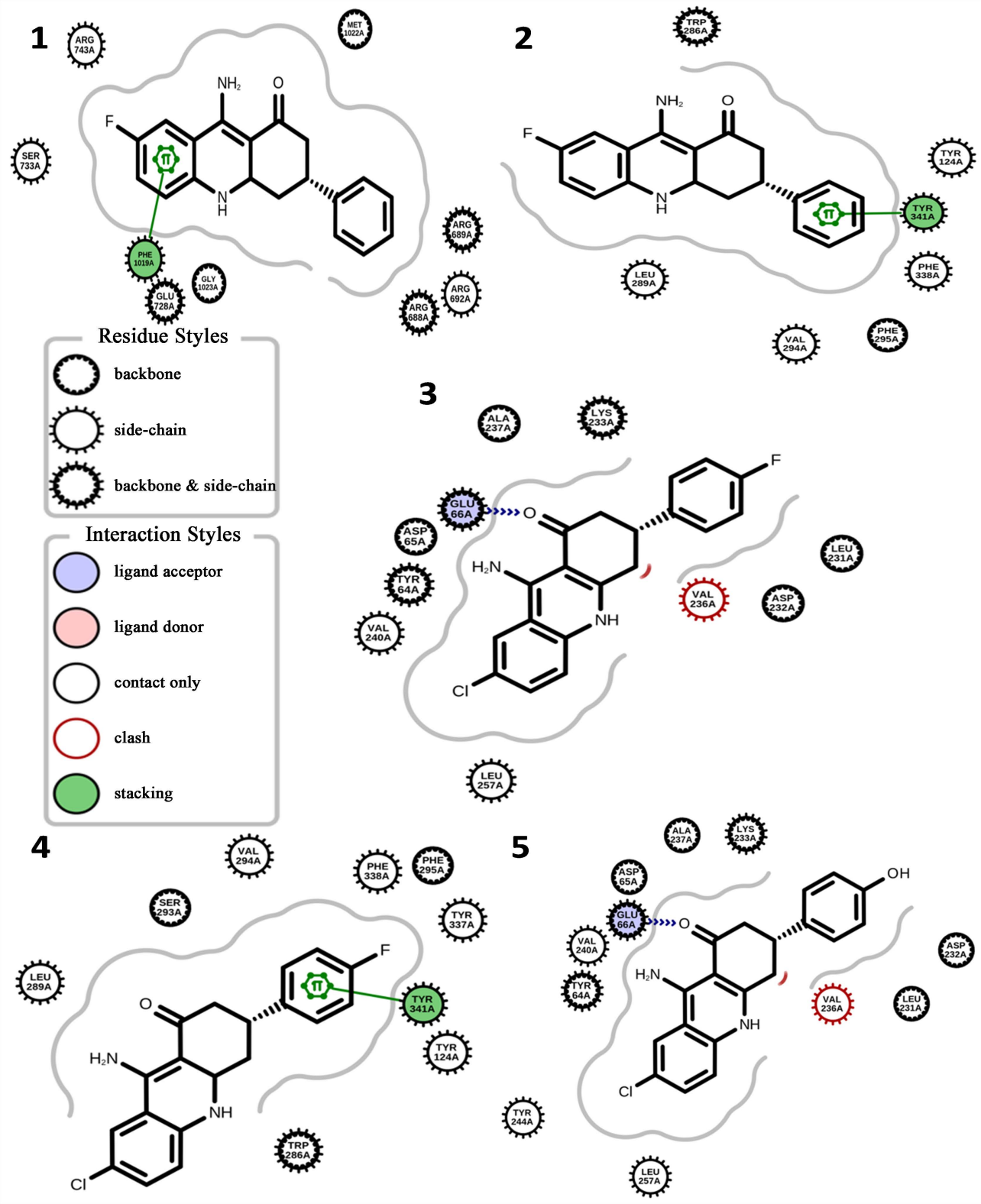

Figure 3. Binding interaction of (1) compound 58c and human topoisomerase IIβ (PDB ID: 3QX3). (2) compound 58c and human acetylcholinesterase (PDB ID: 1B41) (3) compound 58g and human topoisomerase IIα (PDB ID: 1ZXM). (4) compound 58g and human acetylcholinesterase (PDB ID: 1B41). (5) compound 58j and human topoisomerase IIα (PDB ID: 1ZXM).

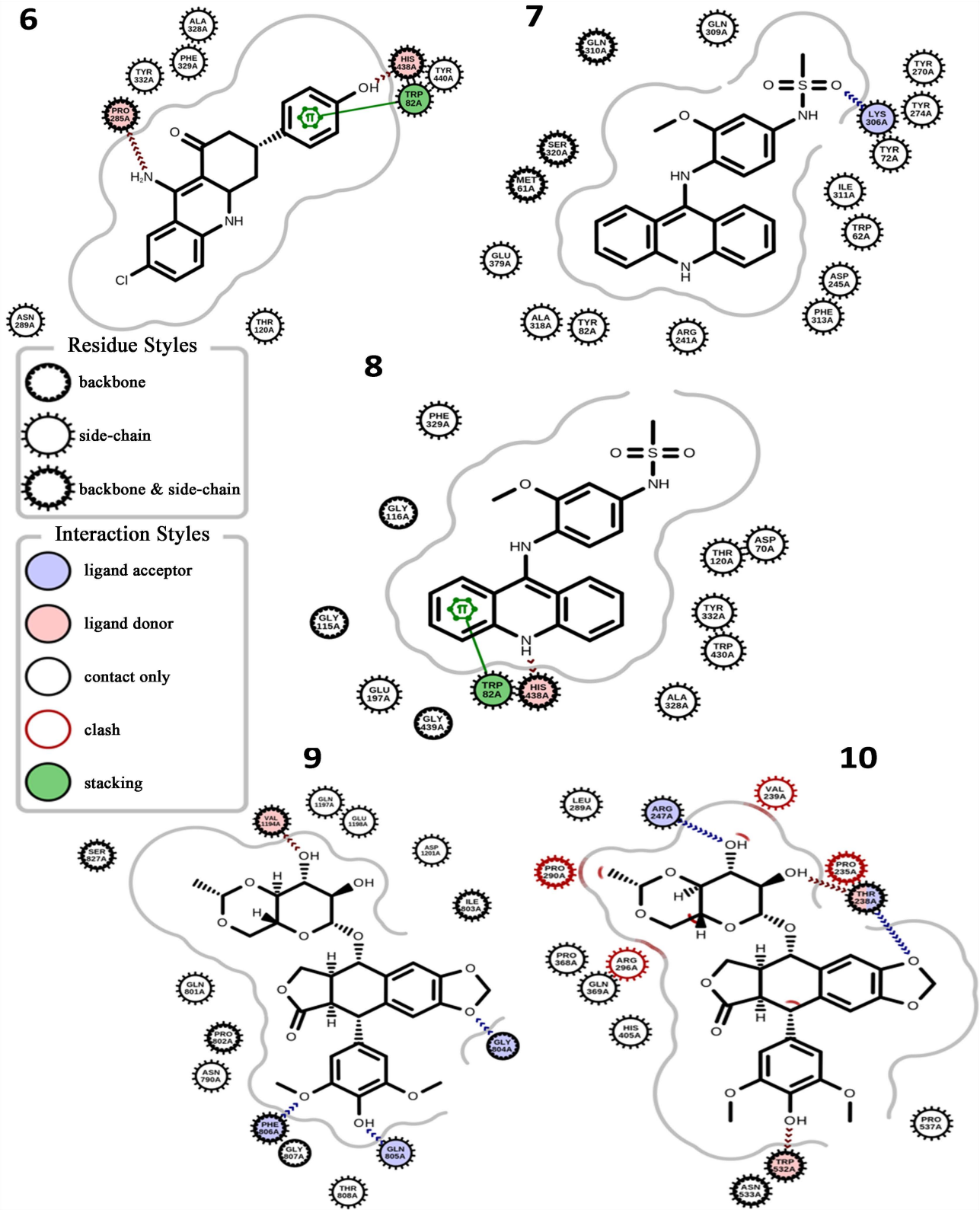

Figure 4. Binding interaction of (6) compound 58j and human butyrylcholinesterase (PDB ID: 6QAC). (7) amscarine and human topoisomerase IIα (PDB ID: 1ZXM). (8) amscarine and human butyrylcholinesterase (PDB ID: 6QAC). (9) etoposide and Human topoisomerase IIβ (PDB ID: 3QX3). (10) etoposide and human acetylcholinesterase (PDB ID: 1B41).

promotes colorectal cancer progression by modulating the tumor suppressor adenomatous polyposis coli (APC), thus impacting WNT/β-catenin pathway [18]. Not all cancer types exhibit high AChE activities, and some of the examples of cancers which possess high AChE activity than normal tissues are: non-small cell lung cancer (NSCLC) such as lung adenocarcinoma, squamous cell lung carcinoma, large cell carcinoma; human leukemias; breast cancer; thyroid cancer, pancreatic cancer, as well as high grade glioma, medulloblastoma and oligodendroglioma [19].

The synthetic compounds investigated in this study have tacrine (9-amino-1,2,3,4-tetrahydroacridine) scaffold in their structure. Tacrine has been found that to be an effective inhibitor of acetylcholinesterase and butyrylcholinesterase, as well serves as a relatively weak catalytic inhibitor of Topo II when compared with 9-aminoacridine [20] [21] [22]. However, tacrine was withdrawn from Alzheimer's disease therapy due to its hepatotoxicity and other detrimental side effects in Alzheimer's disease patients [23]. Tacrine is being currently used as a versatile scaffold in medicinal chemistry for designing novel hybrid compounds with improved pharmacological and toxicological profiles affecting several pathological mechanisms.

Recent studies have explored the anti-cancer activity of tacrine and tacrine-derivatives in human cancer. Roldan-Pena *et al.* [24], synthesized tacrine dimers, sulfide tacrine dimers and selenotacrine dimers and tested their growth-inhibitory activity in a panel of six human cancer cell lines, and the results showed that these tacrine dimers were approximately 10-fold more potent in inhibiting the enzyme activity of AChE than tacrine itself, and in all cell lines the IC_{50} values of the tacrine dimers were approximately 100-fold lower than tacrine and 20-fold lower than standard chemotherapeutic drugs like 5-fluorouracil and cisplatin [24].

It was reported that tacrine-coumarin conjugates containing seven, eight and nine methylene groups in the spacer moiety decreased the viability of human colorectal cancer, breast cancer and mouse mammary carcinoma cells [25]. Small molecule synthetic AChE-inhibitors have many pleiotropic biological effects apart from suppressing AChE activity. Recently, studies show that tacrine and its analogs are not just strong AChE inhibitors they also potently block carbonic anhydrase activity [26], and DNA topoisomerase I and II [27] [28].

The binding of amsacrine to topo IIα is similar to that of etoposide based on the interacting amino acid residues, thus only compounds 58a, 58c, 58f, and 58i showed similar binding, which could be used to infer their anticancer properties. Similar results had been reported for the docking interaction of human topoisomerase IIα (PDB: 1ZXM) with naphthalimide–benzothiazole conjugates and etoposide, which indicated amino acid residues Val57, Gln59, Gln60, Met61, Trp62, Tyr72, Phe77, Pro79, Tyr82, Lys83, Lys306, Gln309, Ile311, Phe313, Ala318, Ser320, Lys321 and Glu379 [29].

The binding of amsacrine to topo IIβ is different from that of etoposide based on the interacting amino acid residues, thus only compounds 58a, 58c, 58f and

58g showed binding similar to that of amsacrine, while compounds 58b, and 58e showed binding similar to that of etoposide. A study has reported that amino acid residues Gly488, Gly506, Ser763, Ser800, Ala801, Ser802, and Pro803, as well as ASP463, Arg487, and Met766 are involve in the Topo II binding interactions near DNA region [30] [31] [32], and it is evident that most of the first-line agents for treating cancer are Topo II poisons, such as etoposide (non-intercalator), and m-amsacrine (intercalator) [5]. A study on novel trifluoromethylated 9-amino-3,4-dihydroacridin-1(2H)-one derivatives has reported that Cl, F, and Br substituted at C7 acted as covalent, rather than interfacial, topoisomerase II poisons and that an amino group at C9 was critical for activity [33]. Thus, compound 58b and 58e could be DNA non-intercalator of topo IIβ while others will be non-Topo II poisons but catalytic inhibitors of topo IIα and topo IIβ.

The binding of amsacrine to acetylcholinesterase is slightly the same with that of etoposide based on the interacting amino acid residues, thus only compounds 58a showed binding property that is different from the standard drugs. Also, binding of amsacrine to butyrylcholinesterase is markedly different from that of etoposide based on the interacting amino acid residues, thus only compounds 58a, 58b, 58d, 58h and 58j showed binding similar to that of amsacrine, while compounds 58c, 58e, 58f, 58g, and 58i showed binding similar to that of etoposide.

A study has observed that there was an increase in AChE expression in the apoptotic cells induced by the DNA topoisomerase inhibitors etoposide or excisanin A, in colon cancer cell line SW620 [34]. Moreover, the implication of 3-phenyl-9-aminoacridone derivatives as anticancer properties will be by inhibition of Topo IIα/β through AChE and BChE pathway, while anti-neurological properties will be by inhibition of Topo IIα/β through neuroligin pathway, although physiological functions of topo IIβ are yet to be fully understood [5] [35] [36] [37].

5. Conclusion

In this study, 10 derivatives of 3-phenyl-9-aminoacridone were synthesized and characterized. The potential pharmacological indications of these compounds were computationally predicted. Overall, the results of this study suggest that the synthetic compounds 58a, 58c, 58f, 58g, and 58i could probably inhibit topo IIα by catalytic inhibition as seen with amsacrine, but only 58b and 58e possessed DNA non-intercalation properties as seen with etoposide, serving as topo II poison. Further work will be done to validate the reported properties of these synthetic compounds on various cancer cell lines; especially those are characterized with high AChE than normal cell.

Acknowledgements

The authors acknowledge the institutional support from the Department of Chemistry, Tennessee State University (USA), Department of Biochemistry,

Vanderbilt University School of Medicine, Grant Number 1R01 GM 126363 (NO), USA, Department of Biochemistry, Federal University Oye-Ekiti (Nigeria).

Conflicts of Interest

The authors declare no conflicts of interest regarding the publication of this paper.

References

[1] Sitki-Copur, M. (2019) State of Cancer Research around the Globe. *Oncology Journal*, **33**, 181-185.

[2] Saini, A., Kumar, M., Bhatt, S., Saini, V. and Malik, A. (2020) Cancer Causes and Treatments. *International Journal of Pharmaceutical Sciences and Research*, **11**, 3121-3134.

[3] Bray, F. and Moller, B. (2006) Predicting the Future Burden of Cancer. *Nature Reviews Cancer*, **6**, 63-74. https://doi.org/10.1038/nrc1781

[4] Czerwinska, P., Mazurek, S. and Wiznerowicz, M. (2017) The Complexity of TRIM28 Contribution to Cancer. *Journal of Biomedical Science*, **24**, Article No. 63. https://doi.org/10.1186/s12929-017-0374-4

[5] Okoro, C.O. and Fatoki, T.H. (2023) A Mini Review of Novel Topoisomerase II Inhibitors as Future Anticancer Agents. *International Journal of Molecular Sciences*, **24**, Article 2532. https://doi.org/10.3390/ijms24032532

[6] Ertan-Bolelli, T. and Bolelli, K. (2019) Discovery of New DNA Topoisomerase II Inhibitors Using Structure Based Virtual Screening Method. *Journal of the Turkish Chemical Society*: *Section A—Chemistry*, **6**, 71-78.

[7] Adeniran, O.Y., Metibemu, A.O. and Boboye, S.O. (2021) Virtual High-Throughput Screening (VHTS), Three-Dimensional Quantitative Structure-Activity and Relationship (3D-QSAR) and Molecular Docking Studies of Novel Phytoinhibtors of Topoisomerase II *α*. *GSC Biological and Pharmaceutical Sciences*, **15**, 72-82. https://doi.org/10.30574/gscbps.2021.15.2.0099

[8] Oyedele, O.S., Bogan, D.N. and Okoro, C.O. (2020) Synthesis, Biological Evaluation and Virtual Screening of Some Acridone Derivatives as Potential Anticancer Agents. *Bioorganic & Medicinal Chemistry*, **28**, Article ID: 115426. https://doi.org/10.1016/j.bmc.2020.115426

[9] Daina, A., Michielin, O. and Zoete, V. (2017) SwissADME: A Free Web Tool to Evaluate Pharmacokinetics, Drug-Likeness and Medicinal Chemistry Friendliness of Small Molecules. *Scientific Report*, **7**, Article No. 42717. https://doi.org/10.1038/srep42717

[10] Pires, D.E., Blundell, T.L. and Ascher, D.B. (2015) pkCSM: Predicting Small-Molecule Pharmacokinetic and Toxicity Properties Using Graph-Based Signatures. *Journal of Medicinal Chemistry*, **58**, 4066-4072. https://doi.org/10.1021/acs.jmedchem.5b00104

[11] Kuhn, M., von Mering, C., Campillos, M., Jensen, L.J. and Bork, P. (2008) STITCH: Interaction Networks of Chemicals and Proteins. *Nucleic Acids Research*, **36**, D684-D688. https://doi.org/10.1093/nar/gkm795

[12] Fatoki, T., Chukwuejim, S., Ibraheem, O., Oke, C., Ejimadu, B., Olaoye, I., Oyegbenro, O., Salami, T., Basorun, R., Oluwadare, O. and Salawudeen, Y. (2022) Harmine

and 7,8-Dihydroxyflavone Synergistically Suitable for Amyotrophic Lateral Sclerosis Management: An in Silico Study. *Research Results in Pharmacology*, **8**, 49-61. https://doi.org/10.3897/rrpharmacology.8.83332

[13] Morris, G.M., Huey, R., Lindstrom, W., Sanner, M.F., Belew, R.K., Goodsell, D.S. and Olson, A.J. (2009) AutoDock4 and AutoDockTools4: Automated Docking with Selective Receptor Flexibility. *Journal of Computational Chemistry*, **30**, 2785-2791. https://doi.org/10.1002/jcc.21256

[14] Trott, O. and Olson, A.J. (2010) AutoDock Vina: Improving the Speed and Accuracy of Docking with a New Scoring Function, Efficient Optimization, and Multithreading. *Journal of Computational Chemistry*, **31**, 455-461. https://doi.org/10.1002/jcc.21334

[15] Eberhardt, J., Santos-Martins, D., Tillack, A.F. and Forli, S. (2021) AutoDock Vina 1.2.0: New Docking Methods, Expanded Force Field, and Python Bindings. *Journal of Chemical Informatics and Modelling*, **61**, 3891-3898. https://doi.org/10.1021/acs.jcim.1c00203

[16] Tao, A., Huang, Y., Shinohara, Y., Caylor, M.L., Pashikanti, S. and Xu, D. (2019) ezCADD: A Rapid 2D/3D Visualization-Enabled Web Modeling Environment for Democratizing Computer-Aided Drug Design. *Journal of Chemical Informatics and Modelling*, **59**, 18-24. https://doi.org/10.1021/acs.jcim.8b00633

[17] Yu, Q., Wang, X., Yang, Y., Chi, P., Huang, J., Qiu, S., Zheng, X. and Chen, X. (2021) Upregulated NLGN1 Predicts Poor Survival in Colorectal Cancer. *BMC Cancer*, **21**, Article No. 884. https://doi.org/10.1186/s12885-021-08621-x

[18] Pergolizzi, M., Bizzozero, L., Maione, F., Maldi, E., Isella, C., Macagno, M., Mariella, E., Alberto Bardelli, A., Medico, E., Marchio, C., Serini, G., Di Nicolantonio, F., Bussolino, F. and Arese, M. (2022) The Neuronal Protein Neuroligin 1 Promotes Colorectal Cancer Progression by Modulating the APC/β-Catenin Pathway. *Journal of Experimental and Clinical Cancer Research*, **41**, Article No. 266. https://doi.org/10.1186/s13046-022-02465-4

[19] Richbart, S.D., Merritt, J.C., Nolan, N.A. and Dasgupta, P. (2021) Acetylcholinesterase and Human Cancers. *Advances in Cancer Research*, **152**, 1-66. https://doi.org/10.1016/bs.acr.2021.05.001

[20] Hunter, A.J., Murray, T.K., Jones, J.A., Cross, A.J. and Green A.R. (1989) The Cholinergic Pharmacology of Tetrahydroaminoacridine *in vivo* and *in vitro*. *British Journal of Pharmacology*, **98**, 79-86. https://doi.org/10.1111/j.1476-5381.1989.tb16865.x

[21] Sabolová, D., Kristian, P. and Kožurková, M. (2018) Multifunctional Properties of Novel Tacrine Congeners: Cholinesterase Inhibition and Cytotoxic Activity. *Journal of Applied Toxicology*, **38**, 1377-1387. https://doi.org/10.1002/jat.3622

[22] Konkolová, E., Hudácová, M., Hamulaková, S., Jendželovský, R., Vargová, J., Ševc, J., Fedorocko, P. and Kožurková, M. (2021) Tacrine-Coumarin Derivatives as Topoisomerase Inhibitors with Antitumor Effects on A549 Human Lung Carcinoma Cancer Cell Lines. *Molecules*, **26**, Article 1133. https://doi.org/10.3390/molecules26041133

[23] Lazarevic-Pasti, T., Leskovac, A., Momic, T., Petrovic, S. and Vasic, V. (2017) Modulators of Acetylcholinesterase Activity: From Alzheimer's Disease to Anti-Cancer Drugs. *Current Medicinal Chemistry*, **24**, 3283-3309. https://doi.org/10.2174/0929867324666170705123509

[24] Roldan-Pena, J.M., Alejandre-Ramos, D., Lopez, O., Maya, I., Lagunes, I., Padron, J.M., Pena-Altamira, L.E., Bartolini, M., Monti, B., Bolognesi, M.L. and Fernan-

dez-Bolanos, J.G. (2017) New Tacrine Dimers with Antioxidant Linkers as Dual Drugs: Anti-Alzheimer's and Antiproliferative Agents. *European Journal of Medicinal Chemistry*, **138**, 761-773. https://doi.org/10.1016/j.ejmech.2017.06.048

[25] Solarova, Z., Kello, M., Hamulakova, S., Ladislav, M. and Solar, P. (2018) Anti-Cancer Effect of Tacrine-Coumarin Derivatives on Diverse Human and Mouse Cancer Cell Lines. *Acta Chimica Slovenica*, **65**, 875-881. https://doi.org/10.17344/acsi.2018.4519

[26] Okten, S., Aydin, A. and Tutar, A. (2019) Determination of Anticancer and Antibacterial Activities of Disubstituted Tacrine Derivatives. *Sakarya University Journal of Science*, **23**, 824-830.

[27] Janockova, J., Plsikova, J., Koval, J., Jendzelovsky, R., Mikes, J., Kasparkova, J., Brabec, V., Hamulakova, S., Fedorocko, P. and Kozurkova, M. (2015) Tacrine Derivatives as Dual Topoisomerase I and II Catalytic Inhibitors. *Bioorganic Chemistry*, **59**, 168-176. https://doi.org/10.1016/j.bioorg.2015.03.002

[28] Skok, Z., Zidar, N., Kikelj, D. and Ilas, J. (2020) Dual Inhibitors of Human DNA Topoisomerase II and Other Cancer-Related Targets. *Journal of Medicinal Chemistry*, **63**, 884-904. https://doi.org/10.1021/acs.jmedchem.9b00726

[29] Singh, I., Luxami, V., Choudhury, D. and Paul, K. (2022) Synthesis and Photobiological Applications of Naphthalimide-Benzothiazole Conjugates: Cytotoxicity and Topoisomerase IIα Inhibition. *RSC Advances*, **12**, 483-497. https://doi.org/10.1039/D1RA04148G

[30] Li, A.L., Hao, Y., Wang, W.Y., Liu, Q.S., Sun, Y. and Gu, W. (2020) Design, Synthesis, and Anticancer Evaluation of Novel Indole Derivatives of Ursolic Acid as Potential Topoisomerase II Inhibitors. *International Journal of Molecular Sciences*, **21**, Article 2876. https://doi.org/10.3390/ijms21082876

[31] Nemr, M.T.M., Sonousi, A. and Marzouk, A.A. (2020) Design, Synthesis and Antiproliferative Evaluation of New Tricyclic Fused Thiazolopyrimidines Targeting Topoisomerase II: Molecular Docking and Apoptosis Inducing Activity. *Bioorganic Chemistry*, **105**, Article ID: 104446. https://doi.org/10.1016/j.bioorg.2020.104446

[32] Arencibia, J.M., Brindani, N., Franco-Ulloa, S., Nigro, M., Kuriappan, J.A., Ottonello, G., Bertozzi, S.M., Summa, M., Girotto, S., Bertorelli, R., Armirotti, A. and De Vivi, M. (2020) Design, Synthesis, Dynamic Docking, Biochemical Characterization, and *in vivo* Pharmacokinetics Studies of Novel Topoisomerase II Poisons with Promising Antiproliferative Activity. *Journal of Medicinal Chemistry*, **63**, 3508-3521. https://doi.org/10.1021/acs.jmedchem.9b01760

[33] Infante Lara, L., Sledge, A., Laradji, A., Okoro, C.O. and Osheroff, N. (2017) Novel Trifluoromethylated 9-Amino-3, 4-Dihydroacridin-1(2H)-Ones Act as Covalent Poisons of Human Topoisomerase IIα. *Bioorganic and Medicinal Chemistry Letter*, **27**, 586-589. https://doi.org/10.1016/j.bmcl.2016.12.011

[34] Deng, R., Li, W., Guan, Z., Zhou, J.M., Wang, Y., Mei, Y.P., Li, M.T., Feng, G.K., Huang, W., Liu, Z.C., Han, Y., Zeng, Y.X. and Zhu, X.F. (2006) Acetylcholinesterase Expression Mediated by c-Jun-NH2-Terminal Kinase Pathway during Anticancer Drug-Induced Apoptosis. *Oncogene*, **25**, 7070-7077. https://doi.org/10.1038/sj.onc.1209686

[35] Yang, X., Li, W., Prescott, E.D., Burden, S.J. and Wang, J.C. (2000) DNA Topoisomerase IIβ and Neural Development. *Science*, **287**, 131-134. https://doi.org/10.1126/science.287.5450.131

[36] Kozurkova, M., Hamulakova, S., Gazova, Z., Paulikova, H. and Kristian, P. (2011) Neuroactive Multifunctional Tacrine Congeners with Cholinesterase, Anti-Amyloid

Aggregation and Neuroprotective Properties. *Pharmaceuticals*, **4**, 382-418. https://doi.org/10.3390/ph4020382

[37] Mabb, A.M., Kullmann, P.H., Twomey, M.A., Miriyala, J., Philpot, B.D. and Zylka, M.J. (2014) Topoisomerase 1 Inhibition Reversibly Impairs Synaptic Function. *Proceedings of the National Academy of Sciences of the United States of America*, **11**, 17290-17295. https://doi.org/10.1073/pnas.1413204111